Submitted to JOM

Local Electronic Effects and Irradiation Resistance in High-Entropy Alloys

T. Egami[1,2,5], M. Ojha[2], O. Khorgolkhuu[3], D. M. Nicholson[4], and G. M. Stocks[5]

[1] Joint Institute for Neutron Sciences and Department of Materials Science and Engineering, University of Tennessee, Knoxville, TN 37996

[2] Department of Physics and Astronomy, University of Tennessee, Knoxville, TN 37996

[3] Joint Institute for Computational Sciences, University of Tennessee and Oak Ridge National Laboratory, Oak Ridge, TN 37831

[4] Department of Physics, University of North Carolina Asheville, Asheville, NC 28804

[5] Oak Ridge National Laboratory, Oak Ridge, TN 37831

E-mail: egami@utk.edu

Abstract:

High-entropy alloys are multi-component solid solutions in which various elements with different chemistries and sizes occupy the same crystallographic lattice sites. Thus none of the atoms perfectly fit the lattice site, giving rise to considerable local lattice distortions and atomic-level stresses. These characteristics can be beneficial for performance under radiation and in high temperature environment, making them attractive candidates as nuclear materials. We discuss electronic origin of the atomic-level stresses based upon first-principles calculations using density functional theory (DFT) approach.

Introduction

Most metallic alloys used today have one majority component with small additives to improve the properties of a pure element. In contrast high-entropy alloys (HEAs) have a number

of constituent elements in nearly equal portions and resultant increase in configurational entropy stabilizes a single phase solid solution[1-3]. HEAs exhibit very interesting and useful properties, including high strength[4,5], low temperature toughness[6], and irradiation resistance[7-9], making HEAs attractive to various applications. These properties actually are not directly influenced by configurational entropy, except that the phase itself is stabilized by high entropy. They are likely to be more closely related to local structures within these alloys, local lattice distortions[10] in particular. However, so far not much attention has been paid to this aspect. A convenient way to describe such local lattice distortion is the concept of atomic-level stresses and strains[11,12]. In this article we discuss the physical meaning of the atomic-level stresses with respect to the concept of atomic size, and show that they can have a significant role in determining the properties of HEAs, with particular focus on irradiation resistance.

Atomic size and atomic-level pressure

Atomic size is an old and very useful concept widely used in metallurgy[13], chemistry[14,15] and other fields of study, such as metallic glass formation[16]. However, it is an elusive concept that still lacks a rigorous definition. It is empirically determined from known atomic distances in crystalline form of elements or compounds, but often depends on composition, and is only loosely transferrable from one composition to another. After all, an electron density is continuous in a solid, and does not have a sharp minimum between two atoms. For this reason some people tend to dismiss this concept as merely an old semi-classical simplistic idea, useful for hand-waving argument but not rigorously meaningful in the modern world of quantum mechanics. We fervently disagree. In our view it is a real, physically meaningful concept, and by dismissing this concept one would forego an opportunity to unravel important physics in complex systems. For instance the atomic size is the key concept underlining the interpretation of the atomic-level stresses which can be calculated classically[11] or quantum-mechanically[17]. In the following we demonstrate its usefulness in the case of elucidating the properties of HEAs.

The atomic-level stress tensor is defined as[11]

$$\sigma_i^{\alpha\beta} = \frac{1}{\Omega_i} \sum_j f_{ij}^{\alpha} r_{ij}^{\beta} , \qquad (1)$$

where α and β are Cartesian coordinates, Ω_i is the atomic volume of the i-th atom, and f_{ij}^{α} and r_{ij}^{α} are the two-body force and the distance between the atoms i and j. Its trace is the atomic level pressure,

$$p_i = \frac{1}{3} Tr\left(\bar{\bar{\sigma}}_i\right) = \frac{1}{3}\left(\sigma_i^{xx} + \sigma_i^{yy} + \sigma_i^{zz}\right), \tag{2}$$

and the remaining tensor elements correspond to five components of shear stresses, $\tau_{m,i}$. The stress is zero (or equal to the external stress if the stress is applied) only for atoms in an elemental material with all atoms on Bravais lattice sites all of which have an identical environment. In glasses and liquids it is non-zero everywhere, and its magnitude depends on temperature[18,19].

The atomic-level stresses arise because the size and shape of an atom does not fit well to the atomic site[12,16]. To explain this concept more explicitly, we propose the following gedanken experiment. We try to place an atom with the radius R_A into a spherical atomic site in a crystal with the radius of R_H. Firstly, we have to compress or expand the atom by the volume strain,

$$\varepsilon_V^T = \left(\frac{R_H}{R_A}\right)^3 - 1 , \tag{3}$$

so that the atom fits the site without affecting the matrix. Here we assign a positive sign of volume strain for expansion. We then relax the strain on the inserted atom and let the matrix accommodate the size misfit until the balance is achieved. This process can be described approximately by the elasticity theory by Eshelby[20], and the atomic volume strain is reduced to

$$\varepsilon_V^I = \frac{\varepsilon_V^T}{K_\alpha}, \quad K_\alpha = \frac{3(1-\nu)}{2(1-2\nu)} , \tag{4}$$

where ν is the Poisson's ratio[21]. Therefore the atomic-level pressure of the inserted atom is,

$$p^I = \varepsilon_V^I B , \tag{5}$$

where B is the bulk modulus. Therefore when an atom is found to have an atomic-level pressure of p, we can back-track this process to calculate the atomic size of this atom, R_A. The presence of the atomic-level pressure justifies the concept of the atomic size: The ideal atomic size exists, and the pressure is generated when the atom does not fit the atomic site it is placed in. In crystalline alloys, such as HEAs, where different elements occupy the same crystallographic lattice site, atoms are invariably under stress due to misfit in size and shape.

Atomic-level pressure in liquid and crystalline CuZr

It has generally been assumed that in stable crystalline compounds atoms experience no force, and thus the stress on each atom is zero. Often the classical interatomic potentials are constructed with this assumption. We found that this is not necessarily the case[17,22]. Although the net force on each atom is zero the local force between two atoms that determine the stress can be very large. In Fig. 1 we show atomic-level pressure in Cu-Zr in crystalline state (B2 structure) by circles[17]. The calculation was done using the locally self-consistent multiple scattering (LSMS) method using the density functional theory (DFT). The atomic-level pressure, P, in the crystalline CuZr exceeds 100 GPa, a huge value comparable to the bulk modulus (B = 120 GPa).

Fig. 1 also shows the atomic-level pressures on Cu and Zr in the liquid state ($Cu_{50}Zr_{50}$), shown by squares, plotted against local atomic volume[17]. In the liquid the local structure can change to accommodate the atomic size effect. A large atom will have a large number of neighbors and small atom will have a small number of neighbors[23]. Therefore in the alloy liquid the average pressure of each element has to be zero if atoms are neutral. However, in $Cu_{50}Zr_{50}$ pressures are non-zero, and the average pressure for Cu is +37 GPa, whereas that for Zr is -32 GPa. The difference in magnitude between Cu and Zr reflects the volume difference. These pressures originate from charge (electron) transfer from Zr to Cu because of the difference in the Fermi energy (electronegativity), which contributes to the compressive pressure at Cu. The local volume strain (= P/B) is therefore about ±0.3.

These pressures are consistent with their atomic volumes. The average local volumes of Cu and Zr in the liquid were found to be 17.16 and 20.90 $Å^3$. Then the effective radii of Cu and Zr are 1.41 and 1.50 Å, assuming the b.c.c. packing fraction of 0.68, consistent with the B2 structure, whereas the metallic radii of Cu and Zr are 1.28 Å and 1.60 Å. Thus the effective radius of Cu is larger than the metallic radius by 0.13 Å, whereas that of Zr is smaller by 0.10 Å. They are consistent with the volume strain of ±0.3 estimated from the atomic-level pressures, and indicate that they originate from the charge transfer from Zr to Cu.

The atomic-level pressure in crystalline CuZr is +109 GPa for Cu and -109 GPa for Zr. Part of these pressures is due to charge transfer. If we assume that the effect of charge transfer is the same in liquid and in crystal, the purely geometrical pressure in the crystalline CuZr is about

74 GPa, corresponding to the volume strain of 0.62. Now the Cu-Zr distance in the B2 structure is 2.826 Å, smaller than the sum of the metallic radii of Cu and Zr. Thus there is repulsive interaction between the Cu-Zr nearest neighbors, while the second neighbor interaction is attractive. Such a state is commonly seen for the b.c.c. structure in which the second neighbors are only 15% further away than the nearest neighbor. In the b.c.c. structure there are only eight nearest neighbors. But there are six second nearest neighbors not far from the first, so that all fourteen first and second neighbors form the atomic cage. Here the second neighbor distance, 3.263 Å, is only slightly longer than the sum of the metallic radii for Zr (3.20 Å), but is considerably longer than the ideal Cu-Cu distance (2.56 Å). Thus the attraction between Zr atoms is stronger than the attraction between Cu atoms, leaving the Cu atom under compression.

Because Zr is larger than Cu, we can think of the B2 structure to be consisting of the simple cubic lattice of Zr, with Cu occupying the body-centered interstitial site at [0.5, 0.5, 0.5]. Then the lattice constant of Zr in the simple cubic lattice should be a = 3.00 Å, given the effective radius of Zr in CuZr, which is 1.50 Å as discussed above. Therefore the size of the body-center interstitial site is 1.10 Å. When a Cu atom with the radius of 1.28 Å is placed in the body-center site the volume strain is 0.58, consistent with the estimate above, 0.62. This very simple argument based upon the atomic size explains the magnitude of the atomic-level pressure quite well, demonstrating that, after all, the concept of atomic size is quite meaningful, once we take the atomic-level pressure and electronic effect into account.

Atomic-level pressure in high-entropy alloys

A similar calculation was carried out for the multi-element alloys of 3*d* transition metals, FeCoNi and CrFeCoNi[24]. The atomic-level pressures for FeCoNi alloy and CrFeCoNi alloy are shown in Figs. 2 and 3, plotted against local atomic volume. Here the model contains 256 atoms in a supercell, and atoms were randomly mixed without any chemical short-range order. Clearly Ni atoms are under compression in both alloys. In FeCoNi Fe atoms are under tension, whereas in CrFeCoNi Cr atoms are under tension. Co atoms in FeCoNi and Co and Fe atoms in CrFeCoNi have small pressures. The trend reflects the electronegativity differences which cause the charge (electron) transfer from earlier transition metals which have higher Fermi levels to later transition metals with lower Fermi levels. Therefore even though the nominal atomic radii

of these elements are very similar, around 1.25 Å, the effective radii due to charge transfer are different, giving rise to local atomic-level pressure and local lattice distortions. We also calculated the atomic-level pressure for liquids. Just as in the case of CuZr in liquids the pressure due to size mismatch is relaxed, so the pressure represents purely the effects of charge transfer. The average values of the atomic-level pressure and atomic volume for each element in HEA and liquid are shown in Table 1. The local volume strain due to these pressures are of the order of ± 0.1 for FeCoNi and ± 0.2 for CrFeCoNi, corresponding to the variation in the effective size of ± 3 % for FeCoNi and ± 7 % for CrFeCoNi. Because of random occupation of the lattice sites by various elements the local site is distorted, which causes not only the volume stresses but also the shear stress at each site. These stresses will increase the resistance to the motion of lattice dislocations, for instance by increasing the Nabbaro-Pierels stress. It is likely that the increased mechanical strength of HEAs[4-6] is related to this effect of local atomic-level strain resulting in hardening.

Irradiation resistance of high-entropy alloys

Another consequence of the atomic-level stresses and local lattice distortion in HEAs is that they make amorphization of the alloy by particle irradiation easier[25]. Particle irradiation creates vacancy-interstitial (Frenkel) pairs, and if the local lattice distortion due to these Frenkel pairs reaches a critical value the lattice can no longer be maintained and amorphization ensues[25-27]. The critical strain for amorphization is 0.067 for volume strain and 0.093 for shear strain[25]. This value of the critical volume strain is consistent with the critical strain for the glass transition[28] and that for glass formation in binary alloys[16], thus it corresponds to the universal critical strain[29]. Because HEAs already have considerable atomic-level strains, only a small additional strain is required to bring the atomic-level strain to the critical value for amorphization. In addition particle irradiation deposits large amounts of kinetic energy which locally melts the lattice, but the melt re-crystallizes quickly. In HEAs local melting and recrystallization happen more easily, wiping out much of structural defects. For this reason HEAs are self-healing[30].

Indeed HEAs are found to be remarkably irradiation resistant. A model equiatomic ternary alloy, Zr-Hf-Nb, was found to be irradiation resistant up to the dose which induces 10

dpa[7,8]. The CoCrCuFeNi HEA was irradiation resistant up to 40 dpa[9]. These encouraging results make the HEAs attractive as nuclear materials. Metallic glasses are also irradiation resistant[31-33]. However, new generation nuclear reactors are operated at elevated temperatures up to 1000°C. At such temperatures metallic glasses become crystalline and lose their strength. HEAs, on the other hand, are irradiation resistant even at high temperatures. Because of the high degree of disorder HEAs can retain some of the good features of metallic glasses, and yet they endure exposure to high temperatures. For this reason they are likely to be strong candidates for nuclear applications.

Conclusions

High-entropy alloys are characterized not only by their high configurational entropy but by the local lattice distortions due to occupation of the same crystallographic sites by different elements. A useful way to characterize the local lattice distortion theoretically is to calculate the atomic-level stresses. The local stresses, calculated quantum-mechanically using the DFT theory, demonstrate that strong atomic-level pressures are present in HEAs due not only to the differences in the intrinsic atomic sizes but due to charge transfer among the elements reflecting the differences in electronegativity. These stresses must have profound effects on the mechanical properties of HEAs, increasing their strength and improving their resistance to particle irradiation. It is most likely that the good properties of HEAs originate, not from high entropy, but mainly from the high magnitudes of atomic-level stresses in these complex alloys.

Acknowledgment

This work was supported by the Department of Energy, Office of Science, Basic Energy Sciences, Materials Sciences and Engineering Division. Part of this research used resources of the Oak Ridge Leadership Computing Facility at Oak Ridge National Laboratory, which is supported by the Office of Science of the Department of Energy under contract DE-AC05-00OR22725.

References:

1. B. Cantor, et al., *Mater. Sci. Eng. A,* 375-377 (2004) pp. 213-218.

2. J.-W. Yeh, et al., *Adv. Eng. Mater*., 6 (2004) pp. 299-303.
3. C.-Y. Hsu, et al., *Metal. Mater. Trans. A*, 35 (2004) pp. 1465-1469.
4. F. Otto, et al., *Acta Mater.*, 61 (2013) pp. 5743-5755.
5. A. Galli and E. George, *Intermetallics*, 39 (2013) pp. 74-78.
6. B. Gludovatz, et al., *Science*, 345 (2014) pp. 1153-1158.
7. T. Nagase, et al., *Intermetallics*, 26 (2012) pp. 122-130.
8. T. Nagase, et al., *Intermetallics*, 38 (2013) pp. 70-79.
9. T. Nagase, P. D. Rack and T. Egami, *Intermetallics*, 59 (2015) pp. 32-42.
10. W. Guo, W. Dmowski, Ph. Rack, P. Liaw, and T. Egami, *Metall. Mater. Trans. A*, 44 (2013) pp. 1994-1997.
11. T. Egami, K. Maeda, and V. Vitek, *Phil. Mag. A*, 41 (1980) pp. 883-901.
12. T. Egami, *Progr. Mater. Sci.*, 56 (2011) pp. 637- 653.
13. W. Hume-Rothery and H.M. Powell. Z. Krist., 91 (1935) pp. 23-47.
14. L. Pauling, *The nature of the chemical bond* (Cornell Univ. Press, Ithaca, 1960).
15. R.D. Shannon, *Acta Crystall. A*, 32 (1976) pp. 751-767.
16. T. Egami and Y. Waseda, J. Non-Cryst Solids 64 (1984) pp. 113-134.
17. D.M. Nicholson, M. Ojha and T. Egami, *J. Phys.: Condens. Matt.*, 25 (2013) 435505.
18. S.-P. Chen, T. Egami and V. Vitek, *Phys. Rev. B* 37 (1988) pp. 2440-2449.
19. V.A. Levashov, R.S. Aga, J.R. Morris and T. Egami, *Phys. Rev. B*, 78 (2008) 064205.
20. J. D. Eshelby, *Proc. Roy. Soc. London A*, 241 (1957) pp. 376-396.
21. T. Egami and D. Srolovitz, *J. Phys. F*, 24 (1982) pp. 2141-2163.
22. T. Egami, M. Ojha, D. M. Nicholson, D. Louzguine-Luzgin, N. Chen and A. Inoue, *Philos. Mag. A*, 92 (2012) pp. 655-665.
23. T. Egami and S. Aur, *J. Non-Cryst. Solids* 89 (1987) pp. 60-74.
24. O. Khorgolkhuu, M. C. Troparevsky, D. M. Nicholson, G. M. Stocks and T. Egami, unpublished.
25. W. Guo, T. Iwashita and T. Egami, *Acta Mater.*, 68 (2014) pp. 229-237.
26. D.T. Kulp, T. Egami, D.E. Luzzi and V. Vitek, *J. Non-Cryst. Solids* 156-158 (1993) pp. 510-513.
27. P.R. Okamoto, N.Q. Lam and L.E. Rehn, Solid State Phys. 52 (1999) pp. 1-135.
28. T. Egami, S. J. Poon, Z. Zhang and V. Keppens, *Phys. Rev. B*, 76 (2007) 024203

29. T. Egami, *Mater. Sci. Eng. A* 226-228 (1997) pp. 261-267
30. T. Egami, W. Guo, P. D. Rack and T. Nagase, *Met. Mat. Trans. A*, 45 (2014) pp. 180-183.
31. E. A. Kramer and W. L. Johnson, *Appl. Phys. Lett.* 35 (1979) pp. 815-818.
32. D. J. Magagnosc, R. Ehrbar, G. Kumar, M. R. He, J. Schroers and D. S. Gianola, *Scientific Reports* 3, 3 (2013) pp. 16-18.
33. D. J. Magagnosc, G. Kumar, J. Schroers, P. Felfer, J. M. Cairney and D. S. Gianola, *Acta Mater*. 74 (2014) pp. 165-182.

		HEA		Liquid	
Alloy	Element	<p> (GPa)	<V> (Å^3)	<p> (GPa)	<V> (Å^3)
Fe-Co-Ni	Fe	-15.07	11.27		
	Co	-2.11	11.05		
	Ni	18.75	11.21		
Cr-Fe-Co-Ni	Cr	-37.55	11.09		
	Fe	-5.74	11.09		
	Co	9.01	10.94		
	Ni	35.16	11.05		

Table 1. The average pressure and volume for each element in HEA and in liquid.

Figure Captions

Figure 1 Atomic-level pressure for Cu (red) and Zr (blue) in the B2 crystalline state (circles) and in the liquid (squares)[17].

Figure 2 Atomic-level pressure for FeCoNi alloy plotted against local volume[22]. The model consists of 256 atoms. Each symbol represent an atom.

Figure 3 Atomic-level pressure for CrFeCoNi alloy plotted against local volume[22].

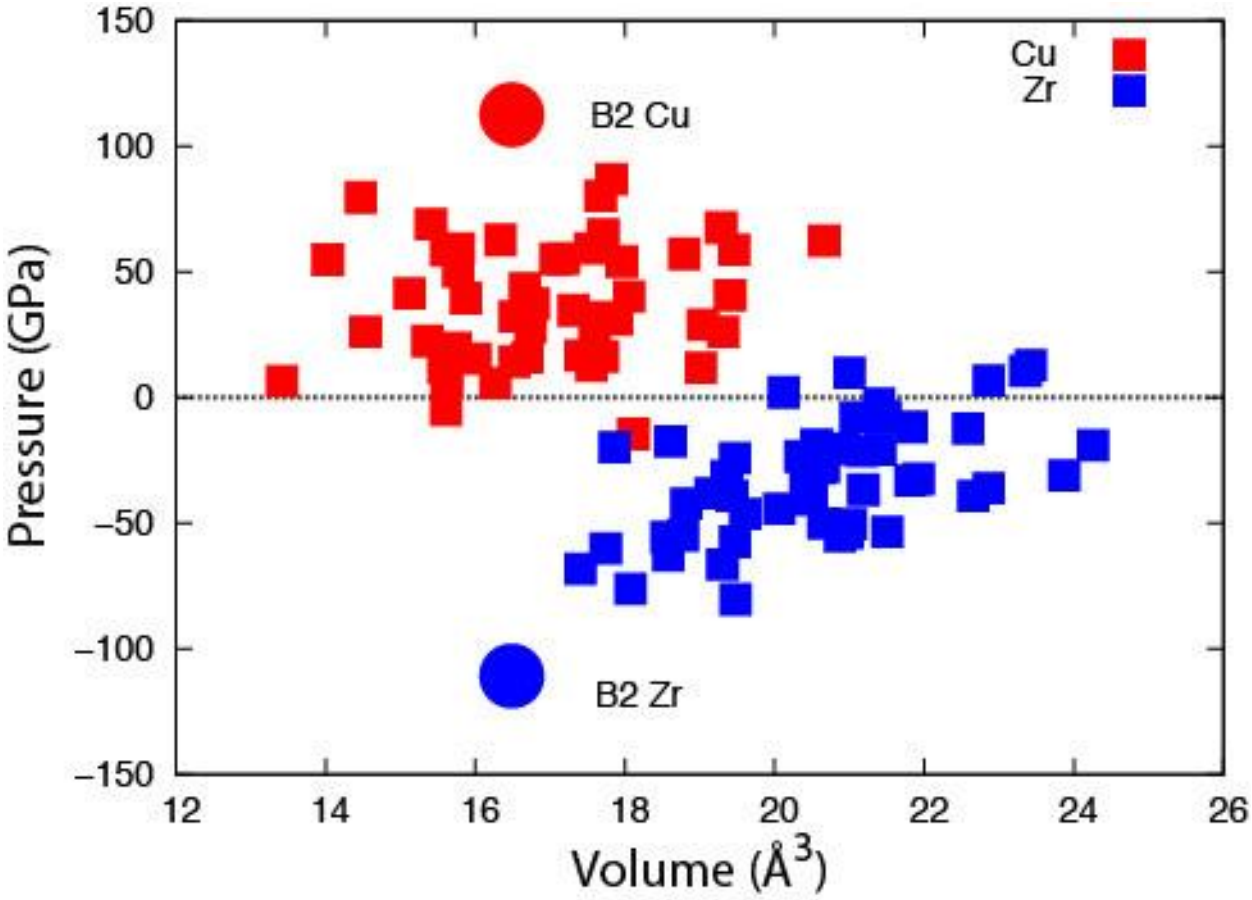
Cu
Zr
B2 Cu
B2 Zr
Pressure (GPa)
Volume (Å^3)
150
100
50
0
−50
−100
−150
12
14
16
18
20
22
24
26

Figure 1

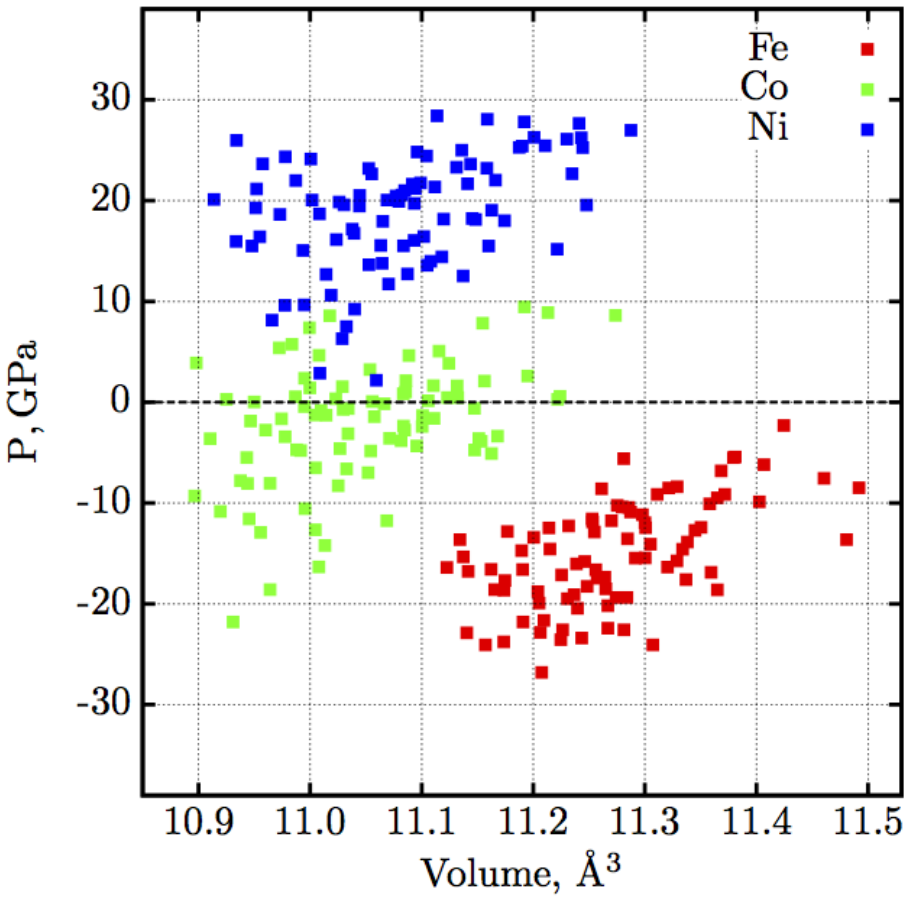
Fe
Co
Ni
30
20
10
0
-10
-20
-30
P, GPa
10.9
11.0
11.1
11.2
11.3
11.4
11.5
Volume, Å³

Figure 2

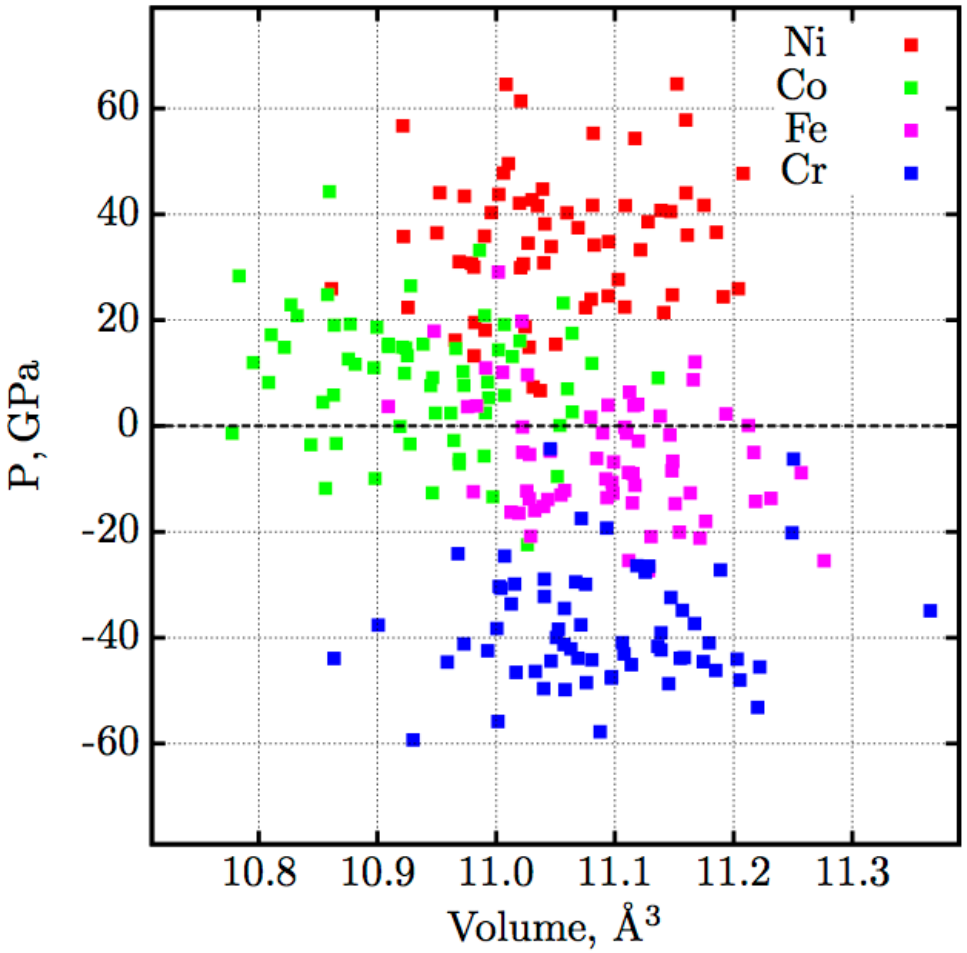
Ni
Co
Fe
Cr
60
40
20
0
-20
-40
-60
P, GPa
10.8
10.9
11.0
11.1
11.2
11.3
Volume, Å³

Figure 3